Preparation and Characterizations of Polycaprolactone/ Green Coconut Fiber Composites

Chin-San Wu

Department of Chemical and Biochemical Engineering, Kao Yuan University, Kaohsiung County, Taiwan 82101, Republic of China

Received 28 January 2009; accepted 14 June 2009
DOI 10.1002/app.30955
Published online 15 September 2009 in Wiley InterScience (www.interscience.wiley.com).

ABSTRACT: The mechanical, thermal, and morphological properties of polycaprolactone (PCL) and green coconut fiber (GCF) composites were evaluated. Blends containing acrylic acid-grafted PCL (PCL-*g*-AA/GCF) exhibited noticeably better mechanical properties due to better compatibility between the two components. The dispersion of GCF in the PCL-*g*-AA matrix was significantly more homogeneous due to the creation of branched and cross-linked macromolecules via reactions between carboxyl groups in PCL-*g*-AA and hydroxyl groups in GCF. The tensile strength of the PCL-*g*-AA/GCF composites at break was considerably greater than that of PCL/GCF composites. In addition, the PCL-*g*-AA/GCF blend was more easily processed due to lower melt viscosity. Biodegradation tests were performed with each composite in an *Acinetobacter baumannii* BCRC 15556 environment. The mass of both composites was reduced by the GCF content within 4 weeks. © 2009 Wiley Periodicals, Inc. J Appl Polym Sci 115: 948–956, 2010

Key words: polyester; natural fiber composites; green coconut fiber

INTRODUCTION

Organic materials such as starch are abundant, inexpensive, renewable, and fully biodegradable. They may be blended with plastics to produce materials with these same properties while retaining some of the desirable properties of the plastic.[1–8] Wood flour (WF), a type of starch, and natural fibers can be incorporated into polymers in relatively high amounts.[9,10] However, blends of plastics and natural fibers typically have poor mechanical properties because the hydrophilic fibers do not adhere well to the hydrophobic synthetic polymer. To solve this problem, reactive functional groups may be incorporated into the synthetic polymer as compatibilizers to enhance the miscibility of the two polymers and improve the mechanical properties of the blend.[11,12] Maleated polypropylene copolymer is an effective compatibilizer in polypropylene/green coconut fiber (PP/GCF) composites,[13] and coupling agents have been used to increase the compatibility of a poly(vinyl chloride)/bamboo flour composites.[14]

Although recycling can solve disposal issues for some plastics, most are irrecoverable and end up in municipal landfills. It is becoming increasingly difficult to find available landfill sites, and there are a host of additional environmental problems associated with the disposal of plastics. To reduce dependence on landfills, the development of biodegradable polymers has received considerable attention. Polycaprolactone (PCL), noted for its flexibility and biodegradability,[15,16] has been blended with other polymers as an ideal packaging material and has been proposed for use in biomedical applications, including catheters, blood bags, and packaging.[17,18] The good biocompatibility between PCL and its copolymers has led to commercially successful applications, as with other aliphatic polyesters.[19,20] Unfortunately, PCL is an expensive plastic. One way of reducing the cost is to blend PCL with natural biomaterials. Hence, a blend of PCL and GCF would appear to offer advantages in both biocompatibility and cost.[21] This study characterizes the physical properties and biodegradability of green coconut fibers (GCF) blended with PCL and acrylic acid-grafted PCL (PCL-*g*-AA). Dried GCF has been widely used in thermoplastic composites. GCF fibers ranging in length from millimeters to a centimeter do not mix well in polypropylene matrices.[22] In contrast to polypropylene, which requires a compatibilizing agent to wet the fibers, the higher hydrophilicity of PCL allows it to naturally wet the GCF fibers.

Many past studies have focused on creating new materials by blending synthetic plastics with biodegradable biopolymers such as starch, cellulose, PCL, polylactic acid, and natural fibers.[23,24] There is also growing interest in exploiting renewable resources as raw materials in the production of biodegradable polymers.[25] Several researchers have successfully

Correspondence to: C.-S. Wu (cws1222@cc.kyu.edu.tw).

developed composites composed of thermoplastic polymers and cellulose-lignin products, such as wood flour (WF). Although cellulose fibers in plastic composites can yield many desirable properties, fiber dispersion and fiber-matrix compatibility remain problematic. Although composites with high fiber content are inexpensive, the high viscosity and other false rheological effects during processing limit the application of these materials.

In this study, the structural and thermal effects of replacing pure PCL with a more compatible acrylic acid-grafted-PCL (PCL-*g*-AA) in GCF-containing composites were systematically investigated. The composites were characterized using Fourier transform infrared (FTIR) spectroscopy, ^{13}C nuclear magnetic resonance (NMR), and differential scanning calorimetry (DSC) to identify bulk structural changes induced by the acrylic acid moiety. In addition, water resistance and the biodegradability of the blends were assessed by measuring the water absorption and weight loss of samples buried in soil inoculated with *Acinetobacter baumannii*.

EXPERIMENTAL

Microbiological sample preparation

Acinetobacter baumannii BCRC 15556 was supplied by the Bioresource Collection and Research Center in Taiwan. The BCRC 15556 strain was cultivated at 37°C and 200 rpm in Nutrient broth (NB) (Difco). The broth consisted of 3 g beef extract, 5 g peptone, 15 g agar, and 1.0 L distilled water at a pH of 7.0. The culture was collected in its early stationary phase for cell entrapment.

Materials

Polycaprolactone (PCL, CAPA 6800), weight average molecular weight 80,000 g/mol, was supplied by Solvay. Acrylic acid (AA) was purchased from Aldrich and purified before use by recrystallization in chloroform. Benzoyl peroxide (BPO) was purified by dissolution in chloroform and recrystallized in methanol. Other reagents were purified using the conventional methods. Referring to the procedures described by Wu,[21] the PCL-*g*-AA copolymer was made in our laboratory, and its grafting percentage was about 6.1 wt %. GCF was obtained from Pingtung.

Sample preparation

PCL-g-AA copolymer

Acrylic acid was grafted onto molten PCL in a nitrogen atmosphere at 85°C ± 2°C. Xylene was used as an interface agent, and the polymerization reaction was initiated with BPO. The reaction was stirred at 60 rpm for 6 h. The reaction product (4 g) was dissolved in 200 mL refluxing xylene at 85°C and extracted five times using 600 mL cold acetone for each extraction. The resultant acetone-insoluble polymer was dried overnight at 80°C and titrated[26] to determine the extent of grafting. The titration showed a grafting percentage of about 6.1 wt %. BPO and AA loading were maintained at 0.3 and 10 wt %, respectively.

Green coconut fiber processing

As byproducts of coconut processing, GCFs are largely available in coastal regions of Taiwan. A coconut weighs about 600 g and contains drinkable juice between the green outer shell and the hard nut in the middle. Inside the coconut is a white fibrous material about 3–5 cm thick. A sample of this material (600 g) was blended and dried in a reactor under vacuum (less than 10 mbar) at 90°C for 1 h. Sodium methoxide (0.3%) was added to the reactor, and the reaction was quenched after ~ 30 min by adding water at 70–80°C. The product was washed five times and dried for 50 min under vacuum. After drying, the middle core contained long yellow fibers of up to 8 cm long. The green outer shell was dried and ground and the resulting fibers sorted. GCF samples obtained before grinding consisted of a mixture of fine brown powder with dispersed yellow-orange single fibers up to 3–5 cm long. The specific gravity of this material was 1.18. The samples were sieved through a mesh, air-dried for 24 h at 70–80°C, and then vacuum dried for at least 2 h at 115°C until the moisture content reached 5 ± 1%.

Composite preparation

Before blending, the GCF samples were cleaned with acetone and dried in an oven at 105°C for 24 h. Composites were prepared in a Brabender "Plastograph" 200-Nm Mixer W50EHT with a blade rotor. The composites were mixed for 15 min between 100 and 110°C with a rotor speed of 50 rpm. The mass ratios of GCF to PCL or to PCL-*g*-AA were set at 5/95, 10/90, 15/85, and 20/80. Residual AA in the PCL-*g*-AA reaction mixture was removed by acetone extraction before the preparation of PCL-*g*-AA/GCF. After blending, the composites were pressed into thin plates using a hot press and put into a dryer for cooling. These thin plates were cut into standard specimens for characterization.

Physical characterization of composites

Measurements

Solid-state NMR spectra were obtained at 50 MHz under cross-polarization while spinning at the magic

angle. Power decoupling conditions were set with a 90° pulse and 4-s cycle time. Infrared spectra of the samples were obtained using a Bio-Rad FTS-7PC FTIR spectrophotometer. The melt temperature (T_m) and enthalpy of melting (ΔH_m) were determined using a TA instrument 2010 calorimeter. DSC sample amounts were between 4 and 6 mg, and the melting curves were recorded from –100 to +120°C at a rate of 10°C/min.

Mechanical testing

An Instron mechanical tester (Model Lloyd, LR5K type) was used to measure tensile strength and elongation at the break of the blends, following standard method ASTM D638. The test films were conditioned at 50 ± 5% relative humidity for 24 h and then tested at a cross-head speed of 20 mm/min. Each blend was tested using five samples, and the results were averaged to obtain a mean value.

Composite morphology

A thin film of each blend was obtained with a hydrolytic press and treated with hot water at 80°C for 24 h before being coated with gold. The surface morphology of these thin films was observed using a scanning electron microscope (Hitachi Microscopy Model S-1400).

Water absorption

Samples were prepared for measuring water absorption by cutting the thin films into 75 × 25-mm strips (150 ± 5 μm thickness) following standard method ASTM D570-81. The samples were dried in a vacuum oven at 50°C ± 2°C for 8 h, cooled in a desiccator, and then immediately weighed to the nearest 0.001 g (this weight was designated W_c). Thereafter, the samples were immersed in distilled water and maintained at 25°C ± 2°C for a 6-week period. During this period, they were removed from the water in 1-week intervals, gently blotted with tissue paper to remove excess water from the surface, immediately weighed to the nearest 0.001 g (this weight was designated W_w), and returned to the water. Each W_w is an average value obtained from three measurements. The percent weight increase due to water absorption (W_f) was calculated to the nearest 0.01% according to eq. 1:

$$W_f\ \% = \frac{W_w - W_c}{W_c} \times 100\% \quad (1)$$

Exposure to *Acinetobacter baumannii*

Samples were cast into films using a 50 × 50-mm plastic mold. Films were removed from the mold and rinsed several times with distilled water until the waste water had a neutral pH. The films were then clamped to a glass sheet and dried in a vacuum oven (50°C ± 2°C, 0.5 mmHg, 24 h). After drying, the films were 0.05 mm ± 0.02 mm thick.

The dried films were placed in compost Petri dishes containing 30-mL NB broth and *Acinetobacter baumannii* BCRC 15556 and incubated at pH 7.0 ± 0.5, 35°C ± 2°C, and 50 ± 5% relative humidity. After incubation, the films were washed extensively with deionized water and dried. Each study was conducted using three replicate test reactors and three replicate samples in each test reactor. Each result is therefore based on nine samples.

RESULTS AND DISCUSSION

Characterization of PCL-*g*-AA/PCL

The FTIR spectra of unmodified PCL and PCL-*g*-AA are shown in Figure 1(A,B). The characteristic transitions of PCL[27] at 3300–3700, 1737, 1725, 850–1480, and 720 cm^{-1} appeared in the spectra of both polymers, with an extra shoulder observed at 1710 cm^{-1} in the modified PCL spectrum, characteristic of —C=O. Similar results have been reported previously.[28,29] This shoulder represents free acid in the modified polymer and therefore indicates the grafting of AA onto PCL. The FTIR spectrum of GCF [Fig. 1(E)] exhibited peaks at 3242 and 1060 cm^{-1} attributed to hydroxyl groups and —CO stretching, respectively.[30]

Closer inspection of the FTIR spectra between 1700 and 1750 cm^{-1} (Fig. 1) reveals significant differences among the spectra of PCL, PCL-*g*-AA, PCL/GCF (10 wt %), and PCL-*g*-AA/GCF (10 wt %). The PCL spectrum [Fig. 1(A)] showed a strong, broad band at 1725–1750 cm^{-1}, similar to the findings of Wang et al.,[31] corresponding to a —C=O stretching vibration. The FTIR spectrum of PCL-*g*-AA [Fig. 1(B)], however, showed an additional peak at 1710 cm^{-1} caused by the grafting of AA onto PCL. The FTIR spectrum of the PCL/GCF composite (10 wt %) [Fig. 1(C)] showed the broad absorption band of PCL at 1725–1750 cm^{-1}, with an additional absorption peak at 1735 cm^{-1}, which is characteristic of GCF.[32,33] The spectrum of PCL-*g*-AA/GCF (10 wt %) [Fig. 1(D)] exhibited a fourth peak at 1743 cm^{-1}. A comparison of the spectra in Figure 1(C,D) suggests that this peak is the characteristic GCF peak, which shifted from 1735 cm^{-1}. This shift was possibly due to the formation of ester carbonyl groups by reactions between the —OH groups of GCF and the —COOH groups of PCL-*g*-AA. This is supported by Oksman and Clemons,[34] in which the FTIR spectrum of an ester carbonyl contained an absorption peak at 1743 cm^{-1}. On the basis of these

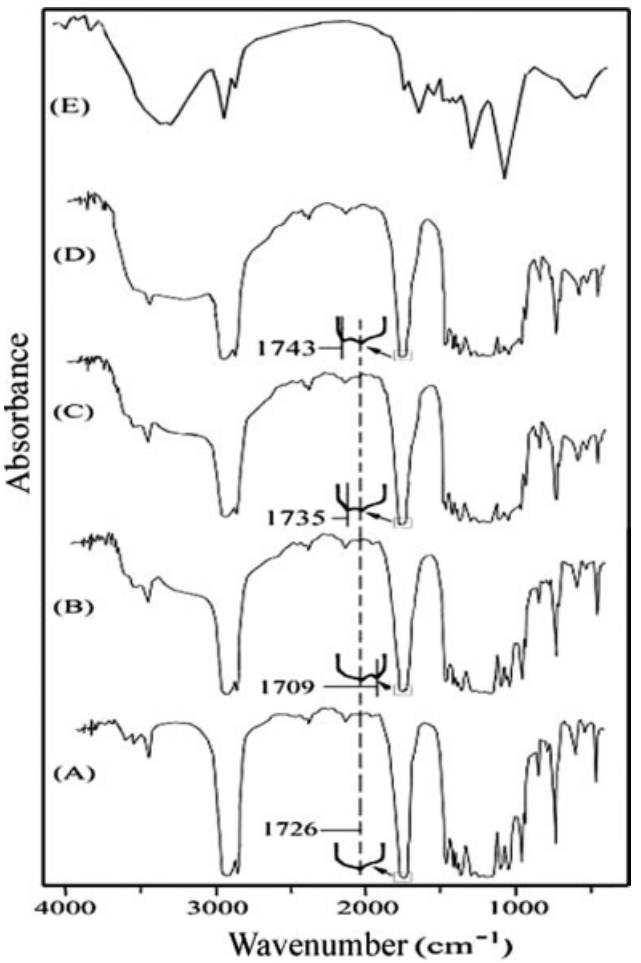

Figure 1 FTIR spectra in the vicinity of C—O and C=O bending deformations for (A) PCL, (B) PCL-*g*-AA, (C) PCL/GCF (10 wt %), (D) PCL-*g*-AA/GCF (10 wt %), and (E) GCF.

results, it was concluded that reactions between the GCF hydroxyl groups and the carbonyl groups of PCL-*g*-AA resulted in a composite composed of branched and cross-linked macromolecules.

To further confirm the grafting of AA onto PCL, the ^{13}C-NMR spectra of PCL and PCL-*g*-AA are compared in Figure 2(A,B). There were six peaks corresponding to carbon atoms in the unmodified PCL (1: $\delta = 64.2$ ppm; 2: $\delta = 28.9$ ppm; 3: $\delta = 25.9$ ppm; 4: $\delta = 25.0$ ppm; 5: $\delta = 34.3$ ppm; 6: $\delta = 173.1$ ppm). Huang and Yang[35] reported a similar outcome in their study of polybenzoxazine/PCL composites. The ^{13}C-NMR spectrum of PCL-*g*-AA showed additional peaks (7: C_β $\delta = 35.6$ ppm; 8: C_α $\delta = 42.2$ ppm; a: —C=O $\delta = 175.1$ ppm), thus confirming that AA was covalently grafted onto PCL.

The solid-state ^{13}C-NMR spectra of GCF, PCL/GCF (10 wt %), and PCL-*g*-AA/GCF (10 wt %) are shown in Figure 2(C–E). The spectrum of GCF was similar to that reported by Shih.[36] Figure 2C coincides with ^{13}C-NMR results of acylated GCF, as characterized by Shih.[36] As in the unblended PCL samples, additional peaks were observed in the spectra of composites containing PCL-*g*-AA relative to those of unmodified PCL. These additional peaks were located at $\delta = 42.2$ ppm (C_α) and $\delta = 35.6$ ppm (C_β). These same features were observed in previous studies[11,28] and are indicative of the grafting of AA onto PCL. However, the peak at $\delta = 175.1$ ppm (C=O) [shown in Fig. 2(B)], which is also typical of AA grafted onto PCL, was absent in the solid state spectrum of PCL-*g*-AA/GCF (10 wt %). This is likely because of an additional condensation reaction between the —COOH group of AA and the —OH group of GCF causing the peak at $\delta = 175.1$ ppm to split into two bands ($\delta = 178.9$ and 177.3 ppm). This additional reaction converted the fully acylated groups of the original GCF to esters [represented by peaks b and c in Fig. 2(C)]. This reaction did not occur between PCL and GCF, as indicated by the absence of corresponding peaks in the PCL/GCF (10 wt %) spectrum in Figure 2D. The formation of ester groups significantly affects the thermal, mechanical,

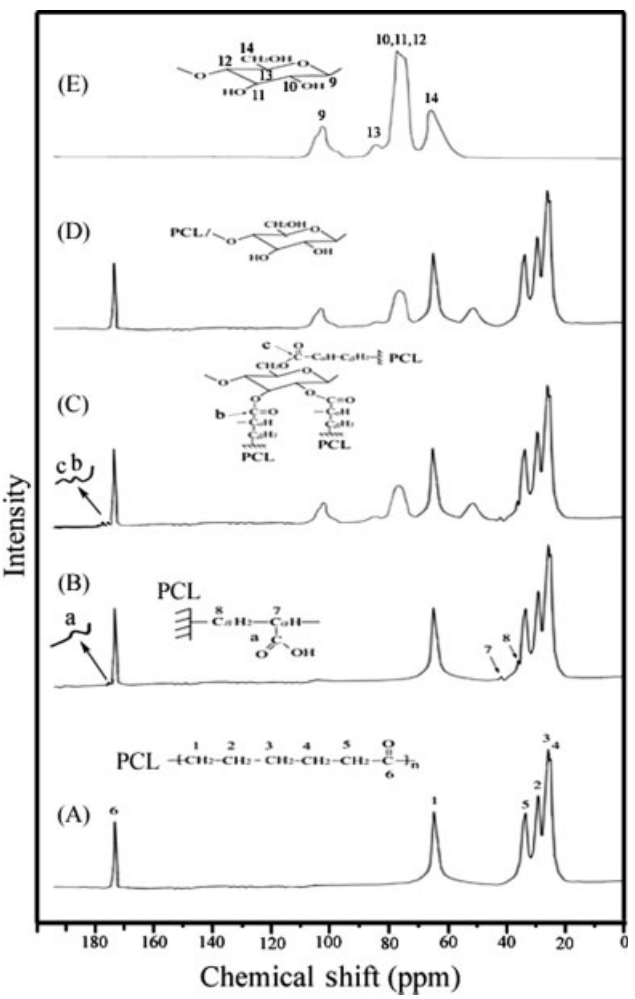

Figure 2 Solid-state ^{13}C-NMR spectra for (A) PCL, (B) PCL-*g*-AA, (C) PCL/GCF (10 wt %), (D) PCL-*g*-AA/GCF (10 wt %), and (E) GCF.

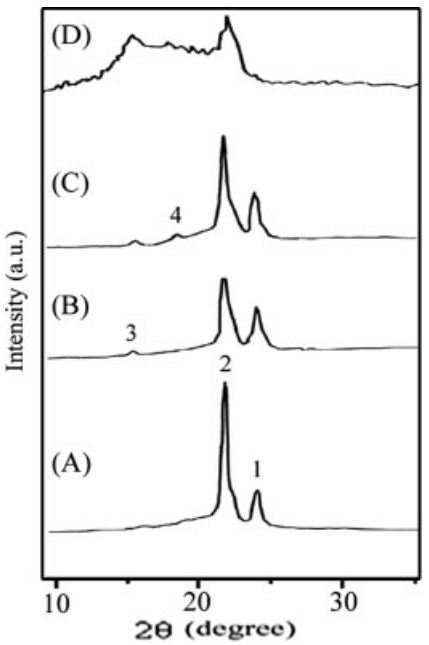

Figure 3 X-ray diffraction patterns for (A) PCL, (B) PCL/GCF, (C) PCL-*g*-AA/GCF, and (D) GCF.

and biodegradation properties of PCL-*g*-AA/GCF and is discussed in greater detail in the following sections.

X-ray diffraction

X-ray diffraction patterns of pure PCL, PCL/GCF (10 wt %), PCL-*g*-AA/GCF (10 wt %) and GCF are shown in Figure 3(A–D). Similar to the results of Ha et al.,[37] pure PCL [Fig. 3(A)] exhibited two diffraction peaks at about 23.7° and 21.2°, designated 1 and 2, respectively. An additional peak was observed for the PCL/GCF composites [Fig. 3(B)] at about 15.1°, designated 3. Peak 3 may have been caused by a change in the coordinate properties of PCL molecules upon blending with GCF,[38,39] indicating that the GCF was physically dispersed throughout the PCL matrix. Figure 3(C) shows an additional peak at 18.2° (designated 4) in diffraction pattern of the PCL-*g*-AA/GCF composites. This peak, also identified by Danyadi et al.,[40] may have been caused by the formation of ester carbonyl groups, indicating that the crystalline structure of the PCL/GCF composites was altered when PCL-*g*-AA was used in place of PCL. Figure 3(D) shows that the XRD pattern of neat GCF contained two peaks at 22.5° and 15.1°. Radiman and Yuliani[41] reported a similar result.

Torque measurements during mixing

The effects of GCF content and mixing time on the melt torque of PCL/GCF and PCL-*g*-AA/GCF composites are shown in Figure 4. When preparing PCL/GCF or PCL-*g*-AA/GCF, the polymer was firstly melted, and then the GCF (fibrous state) was added. Hence, it is the polymer composite containing fibrous filler. Torque values decreased with increasing GCF content and mixing time, approaching a stable value when the mixture was sufficiently mixed after 8 min. The final torque values decreased with increasing GCF content because the melt viscosity of PCL/GCF or PCL-*g*-AA/GCF was lower than that of either PCL or PCL-*g*-AA. Thus, the melt viscosity of the entire composites was reduced. In addition, the melt torque values of the PCL-*g*-AA/GCF composites were significantly lower than those of PCL/GCF composites at the same GCF content. According to Aburto et al.,[42] this improved rheological behavior is due to the formation of ester carbonyl groups (as discussed earlier), which led to conformational changes in the GCF molecule. Sagar and Merrill[43] showed that the melt viscosity of other esterified starches decreased with increasing molecular weight of the ester group.

Differential scanning calorimetry

The heats of fusion (ΔH_f) and melt temperatures (T_m) of PCL/GCF and PCL-*g*-AA/GCF blends with different GCF content were determined from DSC heating thermograms (not shown here) and are shown in Table I. For both composites, T_m decreased with increasing GCF content (Table I), presumably due to the aforementioned decreasing melt viscosity. At the same GCF content, the PCL/GCF blend had a higher T_m than the PCL-*g*-AA/GCF composites (Table I). This result is consistent with the corresponding torque measurements in Figure 4. The

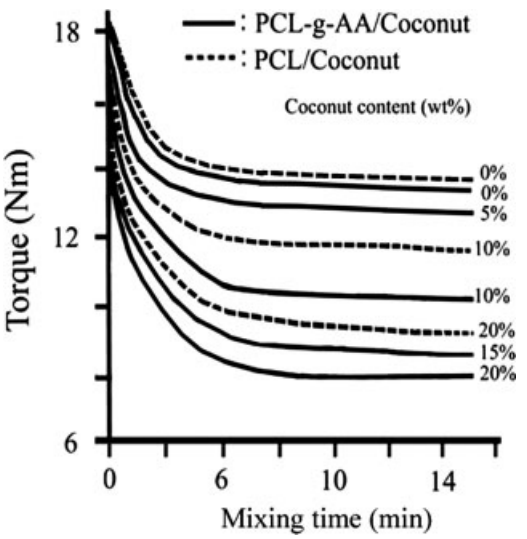

Figure 4 Torque values as a function of mixing time for PCL/GCF and PCL-*g*-AA/GCF blends at various levels of GCF content.

TABLE I
Effect of GCF Content on the Thermal Properties of PCL/GCF and PCL-*g*-AA/GCF Composites

	PCL/GCF			PCL-*g*-AA/GCF		
GCF (wt %)	T_g (°C)	T_m (°C)	ΔH_m (J/g)	T_g (°C)	T_m (°C)	ΔH_m (J/g)
0	−59.6	62.5	72.5	−58.6	61.3	55.2
5	−57.3	61.6	44.2	−55.2	59.8	47.8
10	−54.6	60.0	36.6	−50.6	58.2	41.8
15	−53.1	59.1	29.6	−49.3	57.8	37.6
20	−52.2	58.7	21.8	−48.2	57.3	32.9

lower melt viscosity indicates that PCL-*g*-AA/GCF is more easily processed than PCL/GCF. The glass transition temperature (T_g), shown in Table I, increased with increasing GCF content for both PCL/GCF and PCL-*g*-AA/GCF composites. This increase was likely a result of decreasing space available for molecular motion. T_g values were higher for the PCL-*g*-AA composite by about 1–4°C, suggesting that grafting of acrylic acid to the PCL further restricted molecular motion.

The ΔH_f of pure PCL was 72.5 J/g, whereas that of PCL-*g*-AA was 55.2 J/g (Table I). The lower ΔH_f of PCL-*g*-AA was likely due to the grafted branches, which disrupt the regularity of the chain structures in PCL and increase the spacing between the chains.[41] Values of ΔH_f in PCL-*g*-AA/GCF were ~ 3–12 J/g higher than those of PCL/GCF. These higher ΔH_f values were likely due to the formation of ester carbonyl groups as discussed above.

The ΔH_f may be used as an indicator of the composites crystallinity. Whereas ΔH_f of both PCL/GCF and PCL-*g*-AA/GCF composites decreased with increased GCF content (Table I), the extent of the decrease was significantly greater in PCL/GCF, indicating a lower degree of crystallinity. These results are similar to those for blends of PCL and WF by Wu.[39] The marked decrease in crystallinity of PCL/GCF was most likely a result of hindered motion of the PCL polymer segments due to the presence of GCF in the composite matrix. This can be considered a steric effect because the hydrophilic nature of GCF led to poor dispersibility with the more hydrophobic PCL.[44]

Composite morphology

In most composite materials, effective wetting and uniform dispersion of all components in a given matrix, and strong interfacial adhesion between the phases, are required to obtain a blend with satisfactory mechanical properties. In this study, GCF may be thought of as a dispersed phase within a PCL or PCL-*g*-AA matrix. To evaluate the blend morphology, we employed SEM to examine tensile fractures in the surfaces of PCL/GCF (10 wt %) and PCL-*g*-AA/GCF (10 wt %) samples. The SEM microphotograph of PCL/GCF (10 wt %) in Figure 5(A) shows that the GCF in this blend tended to agglomerate into bundles and was unevenly distributed in the matrix. This poor dispersion was due to the formation of hydrogen bonds between coconut fibers and the disparate hydrophilicities of PCL and GCF. There was also poor wetting in this blend [marked in Fig. 5(A)] due to large differences in surface energy between the GCF and the PCL matrix.[45] The PCL-*g*-AA/GCF (10 wt %) microphotograph in Figure 5(B) shows a more homogeneous dispersion and better wetting of GCF in the PCL-*g*-AA matrix, indicated by the complete coverage of PCL-*g*-AA on the fiber and the removal of both materials when a fiber was pulled from the bulk. This improved interfacial adhesion was due to the similar hydrophilicity of the two components, which allowed

(A)

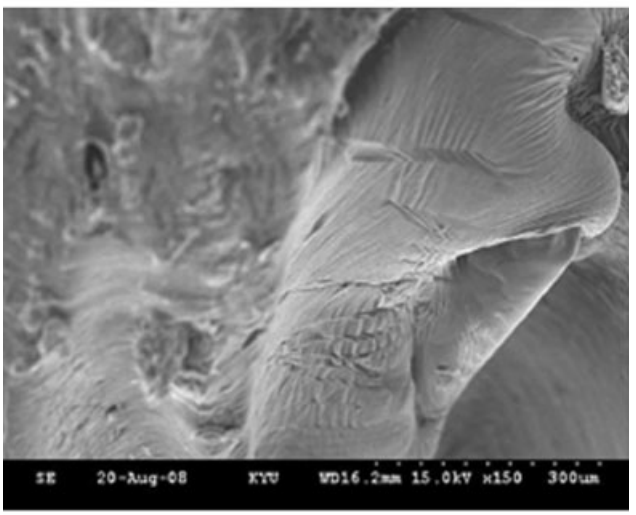

(B)

Figure 5 SEM microphotographs show the distribution and wetting of GCF in PCL/GCF (10 wt %) and PCL-*g*-AA/GCF (10 wt %) composites.

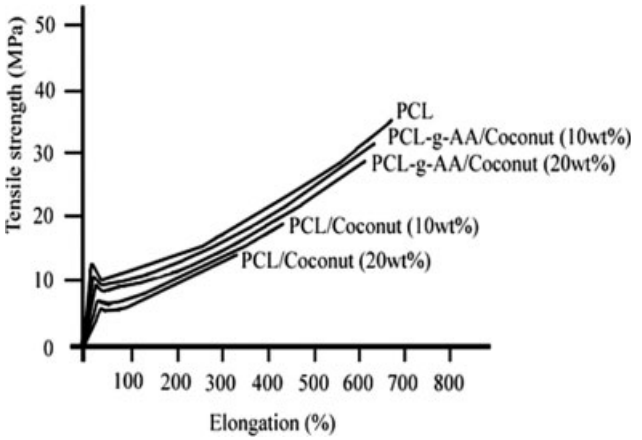

Figure 6 Tensile strength and elongation at break as a function of GCF content for PCL/GCF and PCL-*g*-AA/GCF composites.

for the formation of branched and cross-linked macromolecules and the prevention of hydrogen bonding between coconut fibers.

Mechanical properties

Incompatibility between the two polymers had a great effect on the mechanical properties of the composite. Figure 6 shows the tensile strength and elongation for PCL/GCF and PCL-*g*-AA/GCF blends containing different levels of GCF. Both the tensile strength and elongation decreased when pure PCL was grafted to acrylic acid. For PCL/GCF composites (Fig. 6 and Table II), the tensile strength decreased markedly and continuously with increasing GCF content. This was attributed to poor dispersion of GCF as previously discussed and as shown in Figure 5(A). The tensile strength of PCL-*g*-AA/GCF composites (Fig. 6 and Table II) was significantly higher than that of PCL/GCF composites and increased noticeably with increasing GCF content, despite the lower tensile strength of PCL-*g*-AA relative to pure PCL. In addition, the tensile strength of PCL-*g*-AA/GCF composites was stable at GCF levels greater than 10 wt %. The GCF domain size (the average pore diameter) for each of the composite materials is shown in Figure 7 and Table III. The size of the GCF domains in PCL/GCF increased with increasing amounts of GCF. It is interesting that in PCL/GCF blends containing less than 5 wt % GCF, there was a relatively homogeneous and fine dispersion of GCF in the PCL matrix. The GCF domains observed at 20 wt % GCF provide additional evidence for poor interfacial adhesion and incompatibility between the polymer matrix and the coconut fibers.[46,47]

When PCL-*g*-AA copolymer was added by mixed instrument as a compatibilizer, the GCF domains were reduced. The average pore diameter in PCL/GCF (10 wt %) was 210 μm ± 30 μm compared with the significantly smaller pore diameter of 80 μm ± 18 μm [Fig. 7(A)] in PCL-*g*-AA/GCF (10 wt %) [Fig. 7(B)]. The dispersion of GCF in the PCL-*g*-AA/GCF blends was both fine and homogeneous in all blends up to 20 wt %. The GCF domain size in these highly compatible blends was lower than 100 μm ± 25 μm and was detectable only at higher magnification. The branched and cross-linked macromolecules formed by esterification reactions in the PCL-*g*-AA composites contained components that were compatible with either the PCL or the GCF. This structure allowed these macromolecules to align themselves at the interface of PCL-*g*-AA and GCF during melt blending. The result was a reduction in the interfacial tension between the two polymers and a finer distribution of GCF. These results are similar to those of Nitz et al.,[46] who studied the compatibility of starch in PCL/WF composites and found that compatible blends (using PCL-*g*-MAH as a compatibilizer) yielded smaller pore sizes under tensile disruption.

Although the elongation at break in PCL-*g*-AA/GCF composites was greater than that in PCL/GCF composites (Fig. 6 and Table II), it remained lower than that of pure PCL. For PCL/GCF, the decrease in elongation was attributed to the tendency of GCF to agglomerate into bundles, resulting in poor compatibility between the two phases. The elongation at break in PCL-*g*-AA/GCF composites decreased only moderately with increasing GCF content. These results are similar to those of Lee and Ohkita.[47]

TABLE II
Mechanical Properties of PCL/GCF and PCL-*g*-AA/GCF Composites

	PCL/GCF		PCL-*g*-AA/GCF	
GCF (wt%)	Tensile strength at break (MPa)	Elongation at break (%)	Tensile strength at break (MPa)	Elongation at break (%)
0	37.6 ± 0.7	675 ± 40	35.8 ± 0.8	665 ± 45
5	29.8 ± 1.0	535 ± 45	34.5 ± 0.9	645 ± 40
10	19.6 ± 1.2	450 ± 50	32.6 ± 1.0	630 ± 35
15	17.1 ± 1.4	405 ± 55	30.5 ± 1.1	615 ± 30
20	13.9 ± 1.6	348 ± 58	29.1 ± 1.2	610 ± 28

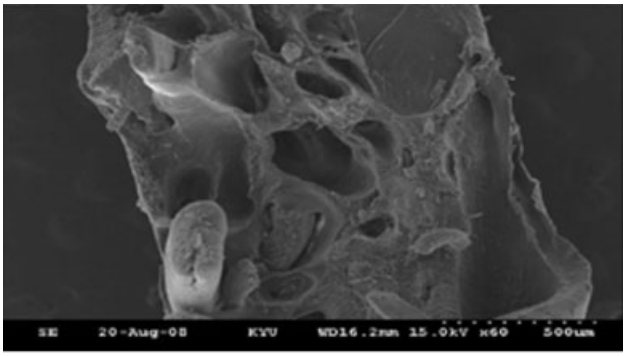

(A)

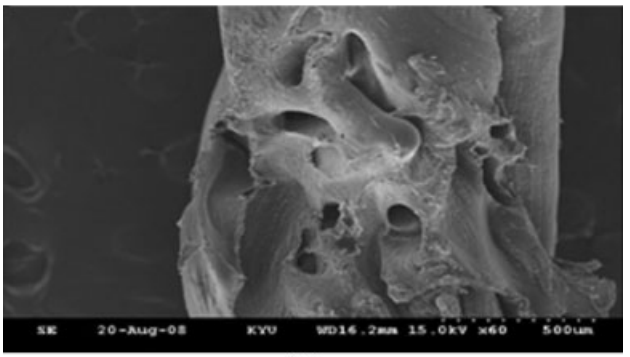

(B)

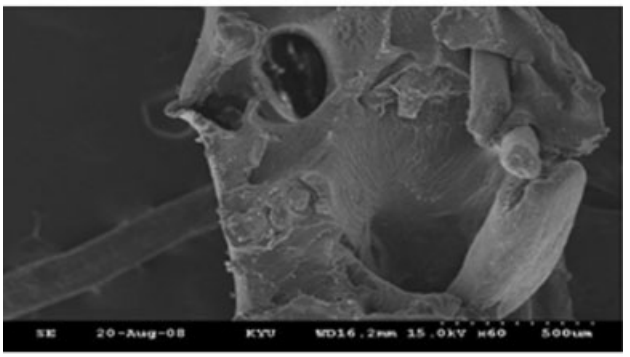

(C)

Figure 7 SEM microphotographs show the domain size of GCF in (A) PCL/GCF (10 wt %), (B) PCL-*g*-AA/GCF (10 wt %), and (C) PCL/GCF (20 wt %).

Compared with pure PCL, the use of PCL-*g*-AA improved both the tensile strength and the elongation at break of the blend. However, the improvement in elongation at break was less than that observed in the tensile strength.

Water absorption

PCL-*g*-AA/GCF composites exhibited moderate water resistance, which was higher than that of PCL/GCF composites at the same GCF content, as shown in Figure 8. Water absorption in PCL and PCL-*g*-AA composites was about 1–3%. For both blends, the percent water gain increased with GCF content. This was attributed to increased hindrance of polymer motion with increasing GCF content due to steric effects of the ester carbonyl and amide functional groups.

TABLE III
The GCF Phase Size of PCL/GCF and PCL-*g*-AA/GCF Composites at Different GCF Contents

	Phase size (μm)	
GCF (wt %)	PCL/GCF	PCL-*g*-AA/GCF
5	150 ± 25	65 ± 15
10	210 ± 30	80 ± 18
15	270 ± 35	90 ± 21
20	310 ± 40	100 ± 25

Biodegradation

Exposure to *Acinetobacter baumannii*

Figure 9 shows the weight change ((degraded sample weight/initial sample weight) × 100%) as a function of time for PCL/GCF and PCL-*g*-AA/GCF composites buried in an *Acinetobacter baumannii* compost. In this environment, water diffused into the polymer sample, causing swelling and enhancing biodegradation. The composites containing a higher percentage of GCF (20%) degraded rapidly over the first 10 weeks, losing a mass equivalent to their approximate GCF content, with a gradual decrease in weight occurring over the next 6 weeks. For both PCL/GCF and PCL-*g*-AA/GCF composites, the degree of weight loss increased with the GCF content. PCL-*g*-AA/GCF exhibited greater weight loss at ~ 5–10 wt %. The mechanical properties of the blends, such as

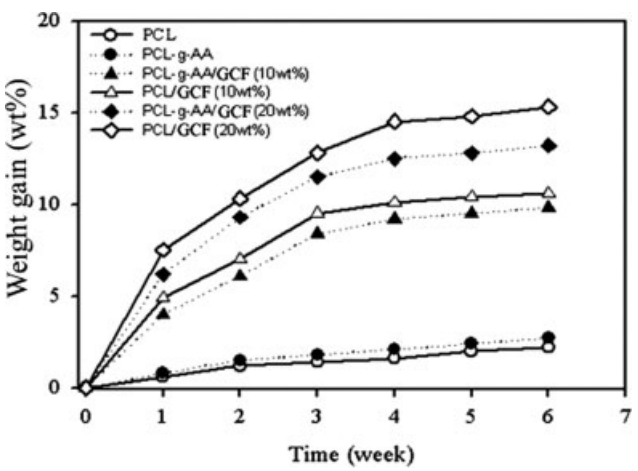

Figure 8 The percent weight gain due to the absorption of water for PCL/GCF and PCL-*g*-AA/GCF blends. The dotted and solid lines indicate the PCL and PCL-*g*-AA composites, respectively, at various GCF levels.

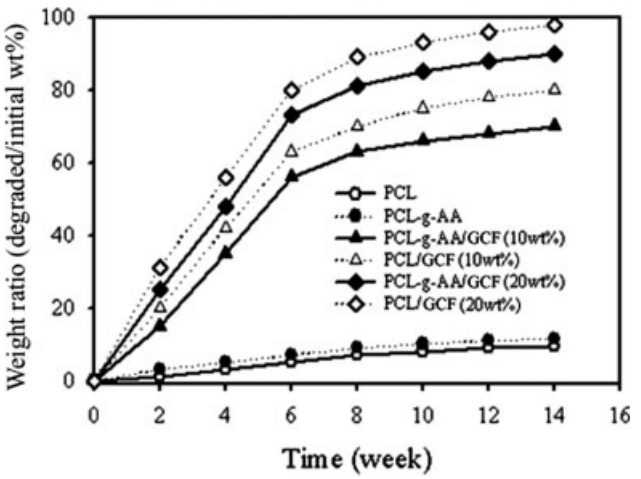

Figure 9 The weight ratios of PCL/GCF and PCL-*g*-AA/GCF samples as a function of time during incubation with *Acinetobacter baumannii*. The dotted and solid lines indicate the PCL and PCL-*g*-AA composites, respectively, at various GCF levels.

tensile strength and elongation at break, also deteriorated after being subject to bacterial degradation.

CONCLUSIONS

The compatibility and mechanical properties of GCF blended with PCL and acrylic acid-modified PCL (PCL-*g*-AA) were examined. FTIR, NMR, and XRD analyses revealed the formation of ester groups due to reactions between —OH groups in GCF and —COOH in PCL-*g*-AA, significantly altering the crystal structure of the composite material. Although DSC tests indicated a decrease in the melting temperatures of both PCL/GCF and PCL-*g*-AA/GCF with increasing GCF content, the PCL-*g*-AA/GCF composites were more easily processed due to lower melt temperatures and mixing torque. The morphology of PCL-*g*-AA/GCF composites was consistent with good adhesion between the GCF phase and the PCL-*g*-AA matrix. In mechanical tests, PCL-*g*-AA enhanced the mechanical properties of the composite, especially the tensile strength. The glass transition temperature of PCL-*g*-AA/GCF was higher than that of PCL/GCF, indicating a more hindered molecular motion. The water resistance of PCL-*g*-AA/GCF was higher than that of PCL/GCF, but when incubated with *Acinetobacter baumannii*, the biodegradation rate was only slightly lower than that of PCL/GCF.

References

1. Pradhan, S. K.; Dwarakadasa, E. S.; Reucroft, P. J. Mater Sci Eng A 2004, 367, 57.
2. Reis, J. M. L. Construct Build Mater 2006, 20, 673.
3. Corradini, E. C.; Morais, L. C.; Rosa, M. F.; Mazzetto, S. E.; Mattoso, L. H. C.; Agnelli, J. A. M. Macromol Symp 2006, 245–246, 558.
4. Rout, J.; Misra, M.; Tripathy, S. S.; Nayak, S. K.; Mohanty, A. K. Polym Compos 2001, 22, 770.
5. Wu, C. S. Macromol Biosci 2005, 5, 352.
6. Fernandes, E. G. Biomacromolecules 2004, 5, 1200.
7. Potente, H.; Reckert, F. Macromol Mater Eng 2002, 287, 791.
8. Cooper, M. A.; Singleton, V. T. J Mol Recognit 2007, 20, 154.
9. Stark, N. M. J Appl Polym Sci 2006, 100, 3131.
10. Leblanc, J. L.; Furtado, C. R. G.; Leite, M. C. A.; Visconte, L. L. Y.; Souza, M. F. J Appl Polym Sci 2007, 106, 3653.
11. Wu, C. S. Polym Degrad Stab 2003, 80, 127.
12. Hristov, V.; Krumova, M.; Michler, G. Macromol Mater Eng 2006, 291, 677.
13. Rozman, H. D.; Tan, K. W.; Kumar, R. N.; Abubakar, A.; Ishak, M. Z. A.; Ismail, H. Eur Polym J 2000, 36, 1483.
14. Kim, J.-Y.; Peck, J. H.; Hwang, S.-H.; Hong, J.; Hong, S. C.; Huh, W.; Lee, S.-W. J Appl Polym Sci 2008, 108, 2654.
15. Nawaby, A. V.; Farah, A. A.; Liao, X.; Pietro, W. J.; Day, M. Biomacromolecules 2005, 6, 2458.
16. Gorna, K.; Polowinski, S.; Gogolewski, S. K. J Polym Sci Part A: Polym Chem 2002, 40, 156.
17. Rhee, S.-H.; Lee, Y.-K.; Lim, B.-S.; Yoo, J. J.; Kim, H. Biomacromolecules 2004, 5, 1575.
18. Sivalingam, G.; Vijayalakshmi, S. P.; Madras, G. Ind Eng Chem Res 2004, 43, 7702.
19. Abou-Zeid, D.-M.; Muller, R.-J.; Deckwer, W.-D. Biomacromolecules 2004, 5, 1687.
20. Sivalingam, G.; Madras, G. Polym Degrad Stab 2004, 84, 393.
21. Wu, C. S. J Appl Polym Sci 2003, 89, 2888.
22. Leblanc, J. L.; Furtado, C. R. G.; Leite, M. C. A.; Visconte, L. L. Y.; Ishizaki, M. H. J Appl Polym Sci 2006, 102, 1922.
23. You, Y.; Lee, S. W.; Youk, J. H.; Min, B. M.; Lee, S. J.; Park, W. H. Polym Degrad Stab 2005, 90, 441.
24. Li, Z.; Zhuang, X. P.; Liu, X. F.; Guan, Y. L.; Yao, K. D. Polymer 2002, 43, 1541.
25. Váquez-Torres, H.; Canché-Escamilla, G.; Cruz-Ramos, C. A. J Appl Polym Sci 1992, 45, 633.
26. Gaylord, N. G.; Mehta, R.; Kumar, V.; Tazi, M. J Appl Polym Sci 1989, 38, 359.
27. Garkhal, K.; Verma, S.; Jonnalagadda, S.; Kumar, N. J Polym Sci Part A: Polym Chem 2007, 45, 2755.
28. Wu, C. S.; Lai, S. M.; Liao H. T. J Appl Polym Sci 2002, 85, 2905.
29. Fumihiko, M.; Shun, M.; Takshi, I. Polym J 1999, 31, 435.
30. Kahlil, H. P. S. A.; Ismail, H.; Rozman, H. D.; Ahmad, M. N. Eur Polym J 2001, 37, 1037.
31. Wang, J.; Cheung, M. K.; Mi, Y. J. Polymer 2002, 43, 1357.
32. Wang, Y.; Yeh, F.-C.; Lai, S.-M.; Chan, H.-C.; Shen, H.-F. Polym Eng Sci 2003, 43, 933.
33. Liao, H. T.; Wu, C. S. J Appl Polym Sci 2003, 88, 1919.
34. Oksman, K.; Clemons, C. J Appl Polym Sci 1998, 67, 1503.
35. Huang, J.-M.; Yang, S.-J. Polymer 2005, 46, 8068.
36. Shih, Y. F. Mater Sci Eng A 2007, 445–446, 289.
37. Ha, J. C.; Kim, S. Y.; Lee, Y. M. J Controlled Release 1999, 62, 381.
38. Nunez, A. J.; Kenny, J. M.; Reboredo, M. M.; Aranguren, M. I.; Marcovich, N. E. Polym Eng Sci 2002, 42, 733.
39. Wu, C. S. J Appl Polym Sci 2004, 94, 1000.
40. Danyadi, L.; Janecska, T.; Szabo, Z.; Nagy, G.; Moczo, J.; Pukanszky, B. Compos Sci Technol 2007, 67, 2838.
41. Radiman, C.; Yuliani, G. Polym Int 2008, 57, 502.
42. Aburto, J.; Thiebaud, S.; Alric, I.; Bikiaris, D.; Prinos, J.; Panayioyou, C. Carbohydr Polym 1997, 34, 101.
43. Sagar, A. D.; Merrill, E. W. J Appl Polym Sci 1995, 58, 1647.
44. Prinos, J.; Bikiaris, D.; Theologidis, S.; Panayioyou, C. Polym Eng Sci 1998, 38, 954.
45. Felix, J. M.; Gatenholm, P. J Appl Polym Sci 1991, 42, 609.
46. Nitz, H.; Semke, H.; Rüdiger, L. J Appl Polym Sci 2001, 81, 1972.
47. Lee, S. H.; Ohkita, T. J Appl Polym Sci 2003, 90, 1900.